Journal of The Electrochemical Society, **157** (4) C146-C156 (2010)
0013-4651/2010/157(4)/C146/11/$28.00 © The Electrochemical Society

Effects of Sodium Chloride Particles, Ozone, UV, and Relative Humidity on Atmospheric Corrosion of Silver

D. Liang,[a] H. C. Allen,[b] G. S. Frankel,[a,*,z] Z. Y. Chen,[d] R. G. Kelly,[d,] Y. Wu,[c] and B. E. Wyslouzil[b,c]**

[a]Department of Materials Science and Engineering, [b]Department of Chemistry, and [c]Department of Chemical and Biomolecular Engineering, The Ohio State University, Columbus, Ohio 43210, USA
[d]Department of Materials Science and Engineering, University of Virginia, Charlottesville, Virginia 22904, USA

The corrosion of Ag contaminated with NaCl particles in gaseous environments containing humidity and ozone was investigated. In particular, the effects of relative humidity and UV light illumination were quantitatively analyzed using a coulometric reduction technique. The atmospheric corrosion of Ag was greatly accelerated in the presence of ozone and UV light. Unlike bare Ag (i.e., with no NaCl particles on the surface), Ag with NaCl exhibited fast corrosion even in the dark, with no UV in the presence of ozone. Samples exposed to different outdoor environments and samples exposed in a salt spray chamber were studied for comparison. Ag corroded at extremely low rates in a salt spray chamber partly because of the combined absence of light and oxidizing agents such as ozone.
 [DOI: 10.1149/1.3310812]

Manuscript submitted November 4, 2009; revised manuscript received January 12, 2010. Published March 12, 2010.

Despite their widespread use, the results of accelerated atmospheric corrosion tests such as ASTM B117 often do not correlate well with field exposures.[1] As shown below, silver is an example of this phenomenon as silver oxidizes readily during outdoor field exposure but is barely attacked in a salt spray chamber. Clearly, some controlling factors of the chemical and electrochemical reactions in the field exposures are not accurately reproduced in the salt spray chamber environment.

Atmospheric corrosion of silver is affected by factors such as relative humidity (RH),[2-4] airborne pollutants,[5,6] and temperature. Traditional atmospheric corrosion studies of Ag have focused mainly on sulfidation[3,7-9] as silver reacts strongly with sulfur-containing species. The absence of such species in the ASTM B117 test is one reason why silver is relatively inert in the salt spray environment. However, there has been little focus on the effects of chloride and photoassisted corrosion.

In a previous paper,[10] the effects of ozone, UV radiation, and RH on the atmospheric corrosion of bare silver were studied. Atomic oxygen generated by the photolysis of ozone by UV radiation reacted quickly with bare silver to form silver oxide. However, 254 nm UV radiation or ozone alone did not cause any corrosion of Ag within the exposure period. The corrosion rate of bare silver was relatively independent of RH, and it was suggested that the initial chemisorption of atomic oxygen or OH radical under wet conditions is relatively unaffected by RH. The effects of chloride on these reactions are not known. Furthermore, the atmospheric corrosion rate of metals in the field is typically dependent on RH as a result of the interactions of water with salts on the surface.[11]

Sea-salt aerosols can play a critical role in the atmospheric corrosion process. Cole et al. described marine aerosol formation, chemistry, reaction with atmospheric gases, transport, deposition onto surfaces, and reaction with surface oxides.[12] The small size of sea-salt aerosols allows them to be carried away by the wind to places far away from the sea.[13] These aerosols are created by physical processes such as the bursting of air bubbles during wave breaking at the surface of the ocean. Sea-salt aerosols can interact with gases in the atmosphere and can absorb gases with large Henry law constants.[12,14] The absorption of SO_2 and HNO_3 acidifies the aerosol and even causes HCl to volatilize. Aerosols commonly contain salts such as NaCl, KCl, $NaSO_4$, $(NH_4)_2SO_4$, $MgCl_2$, $NaNO_3$, and NH_4NO_3.[12]

Ozone (O_3) is an oxidizing agent that is present to varying extents in the atmosphere, with higher concentrations in industrial regions. Ozone has long been added to water in the water purification industry (ozonation process).[15] Ozone reacts with chloride to form Cl_2, and the reaction is strongly influenced by solution pH [16]

$$2H^+ + 2Cl^- + O_3 = O_2 + H_2O + Cl_2 \quad [1]$$

A small amount of OH radicals may form during ozonation of water, but it was reported that the limited amount of OH radicals do not substantially add to the oxidization of chloride ion to molecular chlorine.[15] The reaction mechanism, i.e., via an OH–Cl^- complex or a HO–Cl^- complex, continues to be debated.[17] The rate of Reaction 1 increases with increasing H^+ and Cl^- concentrations. Certain metal ions such as cobalt ions can have catalytic effects on this reaction as the release of Cl_2 gas was observed to increase with increasing concentration of cobalt ions.[18] Moreover, increasing temperature can also increase the reaction rate.[19] Besides Cl_2, the generation of chlorate ions (ClO_3^-) was observed in alkaline media, and the concentration of aqueous ozone decreased with increasing pH as a result of the increased rate in ozone decomposition.[20,21]

The decomposition of aqueous ozone can generate OH radicals through a series of reactions initiated by the reaction of ozone with a hydroxyl anion.[21] After the reaction with OH^-, the decomposition of aqueous ozone can generate reactive species such as the OH radical. However, an OH radical produced during ozonation can barely oxidize chloride to the Cl radical under typical drinking water conditions unless the pH is less than 3.[15] The addition of ozone to chloride solutions can also increase the corrosion potential and breakdown potential of both Cu–30Ni and SS304.[22]

Ozonation with UV radiation at a wavelength of 254 nm is an effective chemical oxidation technique for the treatment of contaminated waters.[23] UV radiation photodecomposes the aqueous ozone to form hydrogen peroxide and molecular oxygen, as shown in Reaction 2. As shown in Reaction 3, UV radiation can further photodecompose hydrogen peroxide and form a hydroxyl (OH) radical, which is a highly oxidizing agent.[23-28] The rates of these reactions depend on the intensity of UV radiation, ozone concentration, and solution pH. The oxidizing power from photolysis and ozonation is higher than ozonation alone due to the generation of a highly reactive OH radical

* Electrochemical Society Fellow.
** Electrochemical Society Active Member.
z E-mail: frankel.10@osu.edu

$$O_3 + H_2O \xrightarrow{h\nu(\lambda=254\ nm)} H_2O_2(aq) + O_2 \quad [2]$$

$$H_2O_2(aq) \xrightarrow{h\nu(\lambda=254\ nm)} 2OH \quad [3]$$

In the absence of water, ozone can interact with UV radiation to generate atomic oxygen, which, like the hydroxyl radical, is also extremely oxidizing[29]

$$O_3 \xrightarrow{h\nu(\lambda<310\ nm)} O + O_2 \quad [4]$$

In this paper, the effects of ozone, UV radiation, and RH on the atmospheric corrosion behavior of Ag with deposited NaCl particles were examined. Smaller size NaCl particles are preferred to simulate the sea-salt particles better, so an approach was investigated to deposit small particles. The corrosion products were analyzed by the galvanostatic reduction method, scanning electron microscopy (SEM), and energy dispersive spectroscopy (EDS). Samples exposed to outdoor environments or in a salt spray chamber were studied for comparison. Possible mechanisms for the atmospheric corrosion of Ag with NaCl, ozone, and UV radiation were proposed.

Experimental

Silver samples of 99.9% purity and 17 × 17 × 2 mm in size were wet-polished to 1 μm and ultrasonically cleaned in analytical grade ethanol for 5 min. The samples were then put into a dessicator for 24 h before exposure. The experimental chamber, UV lamp, ozone generator, and other experimental apparatus were described in a previous paper.[10] Corrosion products generated in the exposure tests were analyzed by the galvanostatic reduction method in a deaerated 0.1 M Na_2SO_4 solution at pH 10 and a current density of −0.1 mA/cm^2 [10] and by other analytical methods such as SEM and EDS.

Field-exposed silver samples were received from Dr. W. Abbott at Battelle Memorial Institute. The samples were exposed at Point Judith, RI for 3 months, West Jefferson, OH for 3 months, Daytona Beach, FL for 3 months, Coconut Island, HI for 1 month, Lyon Arboretum, HI for 1 month, and inland Maine at 3000 ft elevation for 3 months. Details of the exposure site environments are not available. However, Point Judith, Daytona Beach, and Coconut Beach are all seaside exposures, West Jefferson is a rural environment, Lyon Arboretum is a rain forest, and the Maine site is an inland mountaintop. All these samples were first characterized by SEM and EDS, and then some of them were also subjected to X-ray diffraction. The galvanostatic reduction in deaerated 0.1 M Na_2SO_4 solution at pH 10 was conducted on all samples after the characterization.

In the outdoor atmospheric exposure, the samples were exposed to sea-salt aerosols, ozone, and other reactive species under UV radiation. Replicating the details of the atmospheric exposure conditions was very difficult, so a simplified exposure protocol was used for laboratory studies. A high density of very small salt particles was deposited on the sample surface. Upon exposure to an environment with sufficiently high RH, deliquescence resulted in a thin localized electrolyte layer or microdrops on the sample surface. UV light irradiated the sample through a quartz window in the cell, interacting with ozone created by an upstream ozone generator to form atomic oxygen.

A fine distribution of very small salt particles could be achieved by the thermophoretic deposition method,[30] which used a thermal gradient to attract small aerosol particles to the sample surface. Small salt particles were left on the surface upon drying. The thermophoretic deposition apparatus used an aerosol with micrometer-sized NaCl particles that was generated from 0.05 M NaCl solution by a six-jet atomizer. N_2 was used for both the dilution and carrying gas. The NaCl aerosol stream passed through an impactor that removed larger particles from the aerosol. This stream then passed through a copper tube heated to 265°C and then past the sample surface placed normal to the flow of the stream. The sample was attached to a water-cooled holder, creating a thermal gradient that attracted the aerosol particles to the surface.

Nanometer-sized particles could be created by the thermophoretic deposition process, as indicated by the SEM images in Fig. 1. Some particles exhibited a perfect cubic shape. The distribution of these particles was relatively uniform across the sample surface. The size and distribution of these particles were affected by the concentration of the solution in the atomizer, the pressure of carrying gas, the flow rate of dilution gas, the number of atomizer jets used, the deposition time, and the surface roughness. Increasing the atomizer solution concentration resulted in larger particles. Increasing the pressure of carrying gas reduced the evaporation of water in the aerosol particles, thus increasing the ultimate size of the particles. Increasing the flow rate of the dilution gas enhanced the evaporation of the water in the aerosols and decreased the size of the particles. The number of atomizer jets used and the deposition time affected the density of the particles on the sample surface. A rougher surface, e.g., one abraded to 600 grit, had more and larger agglomerations of particles, whereas a surface polished to 1 μm had smaller agglomerations and more individual NaCl particles with diameters of about 100 nm. A long deposition time led to severe particle agglomeration. The salt particle loading was determined by an image analysis of many SEM images of freshly deposited samples. The typical salt particle loading was 4–6 μg/cm^2, achieved by the following set of conditions: 0.05 M NaCl solution, 2 jets, 20 psi carrying gas, 30 L/min dilution gas, and 1.5 h deposition time. The typical distribution of NaCl particle diameters found under these conditions is given in Table I.

Results

Study of particle deliquescence with ESEM.— Deliquescence of thermophoretically deposited NaCl particles was studied using environmental scanning electron microscopy (ESEM). ESEM is capable of imaging surfaces at a much higher pressure than the normal SEM, though at pressures still lower than atmospheric. The SEM images were taken using the gaseous secondary electron detector. It is possible to control the SEM chamber RH to high values by controlling temperature and pressure. A piece of 2 mm thick bare Ag sample was cut to 5.15 × 5.15 mm to fit the sample holder of the ESEM. The sample was polished to 1 μm and was put into a desiccator before the experiment. A layer of NaCl nanometer-sized particles with a relatively uniform size distribution was formed on the surface using the thermophoretic deposition method described above. A video camera recorded the NaCl deliquescence process; the critical RH for the deliquescence of NaCl is about 75%.[31] The RH was increased from low values to 90% by 5% every 2 min to allow equilibration. After 2 min at 90%, the RH was decreased to 70% to watch the recrystallization of NaCl particles from the NaCl microdrops.

Figure 2 shows images taken during this sequence. In Fig. 2a, taken at 50% RH, particles and agglomerations of particles 1 μm can be seen, as well as very fine submicrometer particles. As the RH was increased to 60% and then to 70% RH (Fig. 2b and c), some of the smallest particles disappeared. So, there is evidence for the interaction between water and NaCl, even below the critical RH. At 80% RH, the small particles all vanished, the large cubic crystals were still present but diminished slightly in size, and the large agglomerations were radically altered in shape (Fig. 2d). The polishing scratches on the surface were still visible even at 80% RH. However, at 90% RH, the surface contrast changed sharply (Fig. 2e). The NaCl particles were not visible at all; only contaminant particles remained. The polishing scratches were also not visible. Large dark patches or microdrops of up to 30 μm were evident. Apparently, the relatively thick deliquesced salt layer blocked the electron emission from the sample surface. Upon decreasing the RH back to 70%, the dark areas gradually disappeared and efflorescence resulted in reprecipitation of the NaCl into crystals, most of which were micrometers in size (Fig. 2f). No large hysteresis was observed during this RH

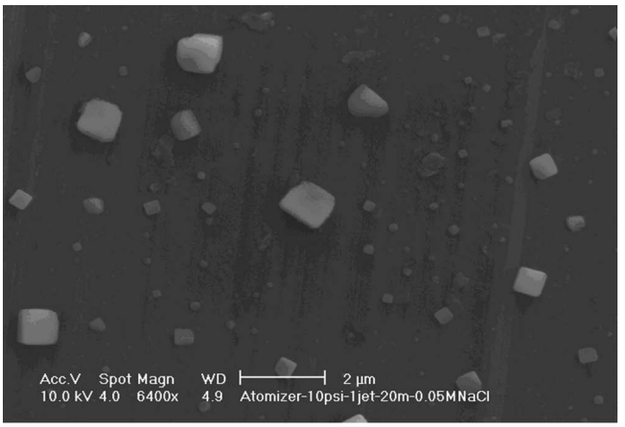

a.

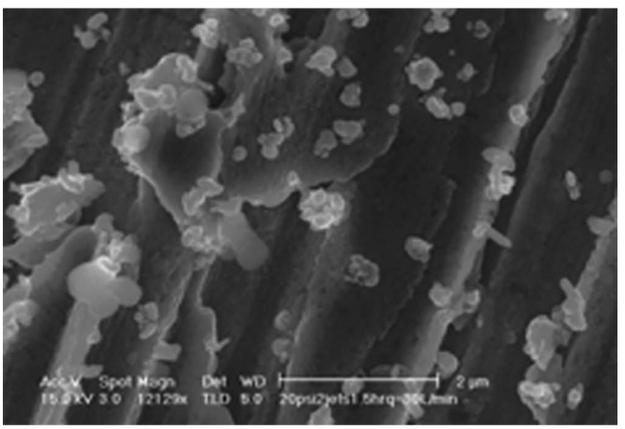

b.

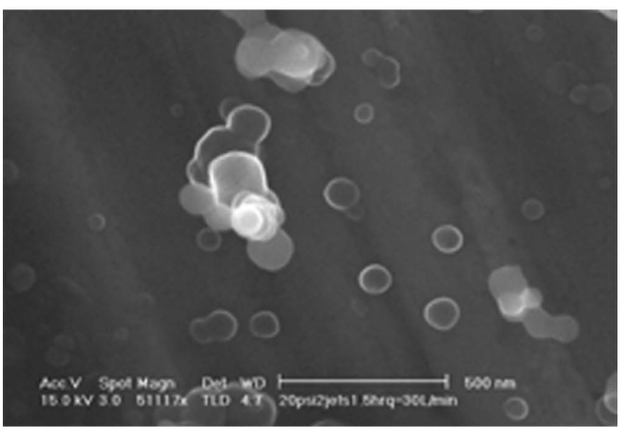

c.

Figure 1. SEM pictures of deposited NaCl particles on samples surface. (a) 1 jet, 10 psi, 10 L/min, 20 min, and marker = 2 μm; (b) 2 jets, 20 psi, 30 L/min, 1.5 h, and marker = 2 μm; (c) 2 jets, 20 psi, 30 L/min, 1.5 h, and marker = 500 nm.

cycle. Natural variations in RH that occur in the environment, such as during diurnal cycles, might result in a similar coarsening of fine aerosol particles on the samples exposed outdoors.

Effects of UV radiation and RH.— As discussed above, UV radiation of proper wavelength can decompose ozone to form reactive

Table I. Typical distribution of NaCl particle size in an area of 15 × 20 μm for the following deposition conditions: 0.05 M NaCl solution, 2 jets, 20 psi carrying gas, 30 L/min dilution gas, and 1.5 h deposition time.

Number	Diameter (nm)
5–10	250
5–10	150
10–20	100

atomic oxygen or OH radical, both of which are able to oxidize bare silver at a fast rate. Previous work has shown that bare silver does not experience fast corrosion when exposed to humidity and ozone in the absence of UV.[10] It was also found that RH had little effect on the corrosion behavior of bare silver in the presence of O_3 and UV radiation.[10] This limited RH effect is because the thin adsorbed water layer formed at RH values less than 100% on the clean Ag surface does not influence the chemisorption of the OH radical and the subsequent oxidation. Hence, it is of interest to understand the effects of UV radiation and RH on the corrosion of silver samples with deposited NaCl particles.

Ag samples with 8 $\mu g/cm^2$ NaCl particles were exposed for 22 h to an environment containing 0.633 ppm O_3 and RH ranging from 0 to 90%, with or without UV irradiation. Samples without UV irradiation were kept in complete darkness. The flow rate of O_2 was 1 cm^3/min, and the total flow rate was controlled at 892 cm^3/min. After the experiments, samples were galvanostatically reduced in deaerated 0.1 M Na_2SO_4 solution at pH 10. Samples both with and without UV irradiation exhibited some level of corrosion as the surface of both samples turned slightly gray after exposure. Figure 3 shows that a layer of corrosion product with crystalline particles was found on both surfaces, and the amount of product seems to be similar at 90% RH for the two cases. The particles were submi-

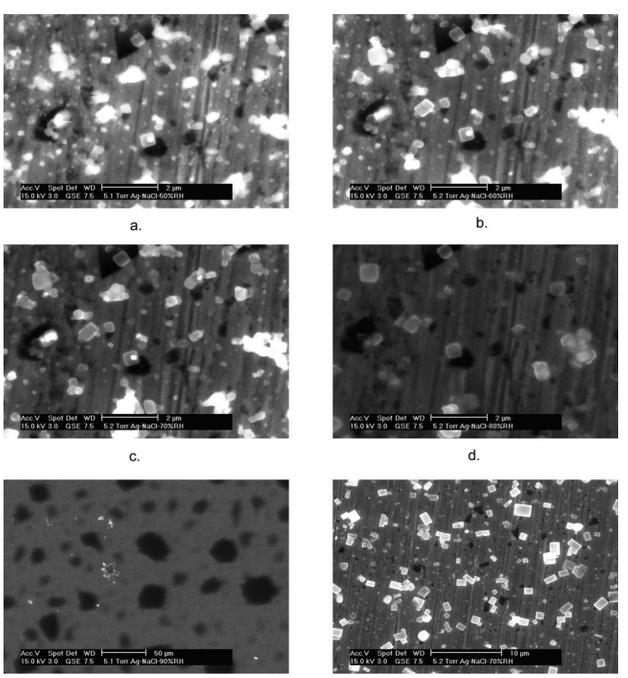

a. b. c. d. e. f.

Figure 2. SEM pictures of NaCl particles at Ag surface under different RHs. (a) 50% RH, marker = 2 μm; (b) 60% RH, marker = 2 μm; (c) 70% RH, marker = 2 μm; (d) 80% RH, marker = 2 μm; (e) 90% RH, marker = 50 μm; (f) RH dropped from 90 to 70%, marker = 10 μm.

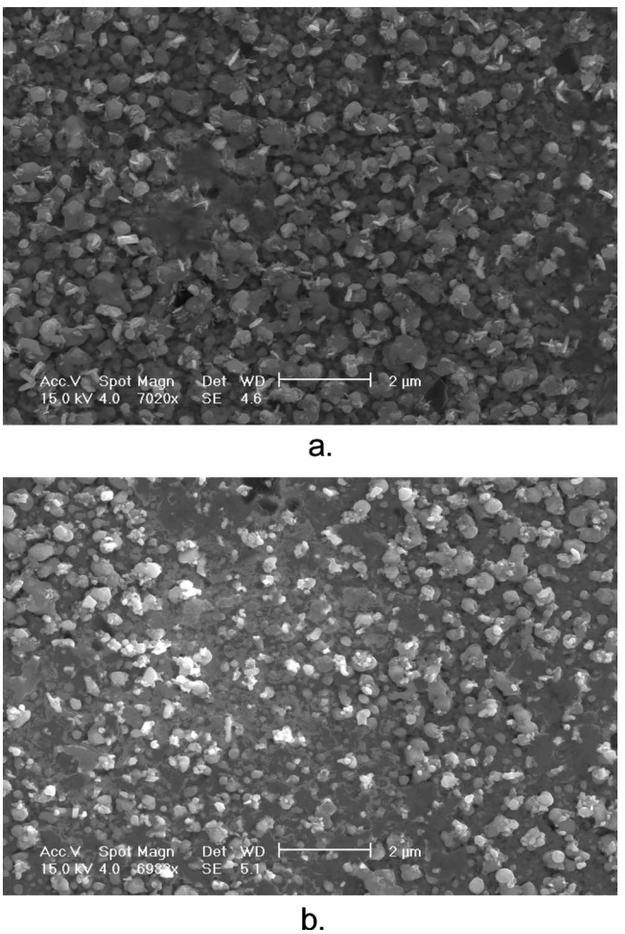

Figure 3. SEM pictures of silver with 8 $\mu g/cm^2$ NaCl in 0.633 ppm O_3, 90% RH environment, after exposure. Micrometer marker = 2 μm (a) with UV radiation and (b) in dark.

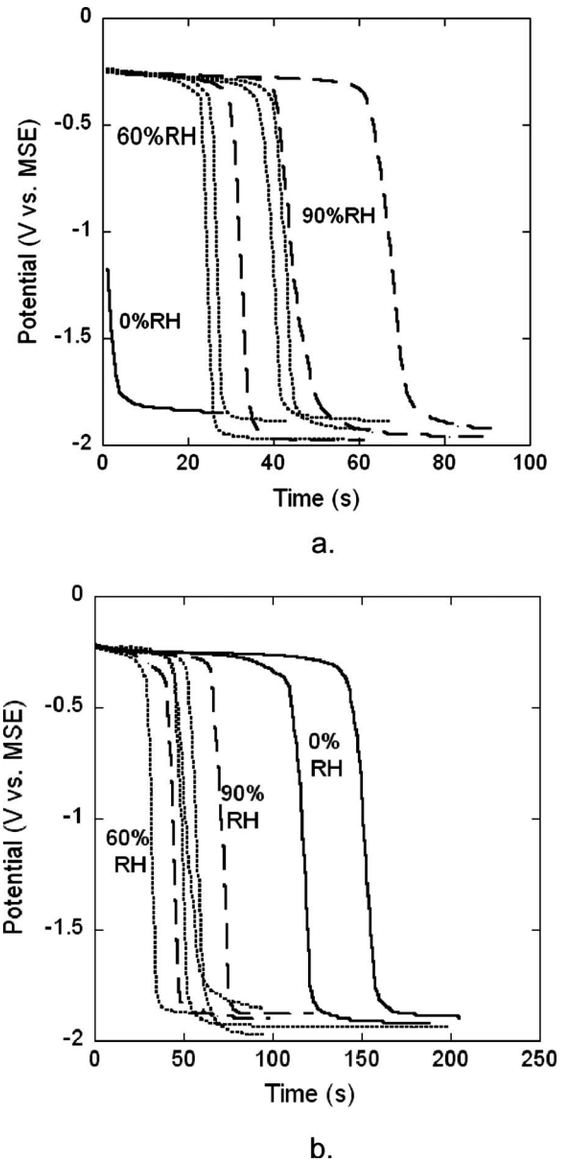

Figure 4. Galvanostatic reduction curves for silver with 8 $\mu g/cm^2$ NaCl in 0.633 ppm O_3 at different RH values for 22 h. Reduction solution is deaerated 0.1 M Na_2SO_4 at pH 10. (a) In dark and (b) with UV radiation.

crometer in size, which are much smaller than the microdrops observed in the ESEM, and corrosion product covered the surface even between the particles. The surface was entirely covered by the corrosion product, and no correlation between the microdrops and corrosion product was found. Figure 4 shows the galvanostatic reduction curves, and Fig. 5 shows the reduction charges for the samples at different RH values and also includes the reduction for bare silver at different RH values for comparison.[10]

A similar amount of corrosion product formed on the NaCl-deposited samples at 90% RH for both UV-irradiated and dark conditions. The average reduction times and charges were 52 and 54 s and 0.0052 and 0.0054 C/cm^2 for samples in the dark and with UV radiation, respectively. Clearly, UV radiation had little effect on the corrosion rate under these conditions. However, the amount of reduction charge for the samples with NaCl particles was less than that for bare Ag exposed to the same concentration of ozone at 90% RH with UV. However, essentially no corrosion product was found on the bare Ag sample under dark conditions, even with ozone and RH.[10]

The reduction charge for the NaCl-deposited samples at 60% RH was lower than that at 90% RH, and the average charge with UV radiation, 0.0048 C/cm^2, was larger than that in the dark, 0.0033 C/cm^2. Because 60% RH is below the critical RH for deliquescence (75% for NaCl), a bulk electrolyte film was not expected to exist on the surface. Similar to the case at 90% RH, the amount of corrosion product for the NaCl-deposited samples was less than that for bare Ag exposed to UV radiation.

Under dry conditions at close to 0% RH, the average reduction charge for the sample with UV radiation increased to 0.0132 C/cm^2, whereas it dropped to essentially zero for the sample in the dark. This behavior at 0% RH was identical to that found for bare Ag, both with UV radiation and in the dark. Because the NaCl-deposited samples at 0% RH behaved like the bare Ag samples, the amount of corrosion product was higher than that for the case at 60% RH.

Effect of ozone.— The effect of O_3 was studied on Ag samples with NaCl particles in the exposure chamber. Figure 6a shows a sample with about 8 $\mu g/cm^2$ NaCl particles exposed for 22 h to 90% RH with UV radiation but no ozone. The surface looked shiny and unchanged, and the galvanostatic reduction curve in deaerated 0.1 M Na_2SO_4 solution at pH 10 indicated no reduction charge (i.e., no corrosion product) in the absence of ozone (Fig. 6b). This environment contained O_2, but the UV radiation at the 254 nm wavelength was not strong enough to break apart O_2 to form reactive atomic oxygen or ozone. Without one of these oxidants, there is no

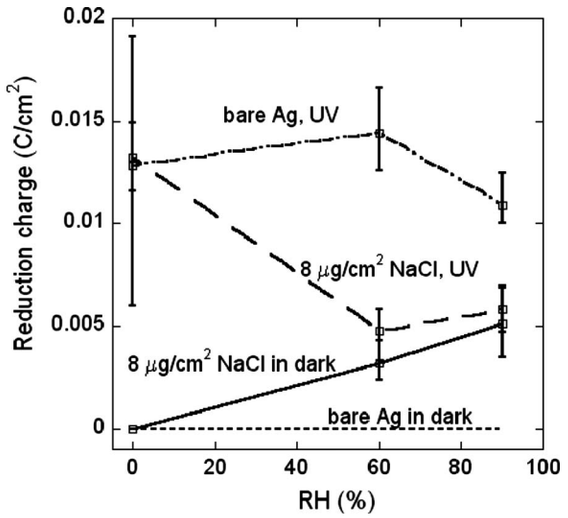

Figure 5. Reduction charge for Ag sample with 8 μg/cm^2 NaCl with and without UV radiation at 0.633 ppm O_3, different RHs for 22 h. Data for bare Ag shown for comparison.[10]

fast corrosion of Ag. This same result was found for bare Ag [10] and is also relevant for NaCl-deposited Ag, even for an RH that is higher than the critical value for deliquescence. If, however, UV radiation of 242 nm wavelength or lower were used, the molecular oxygen would be decomposed to form atomic oxygen and fast corrosion would occur.[10]

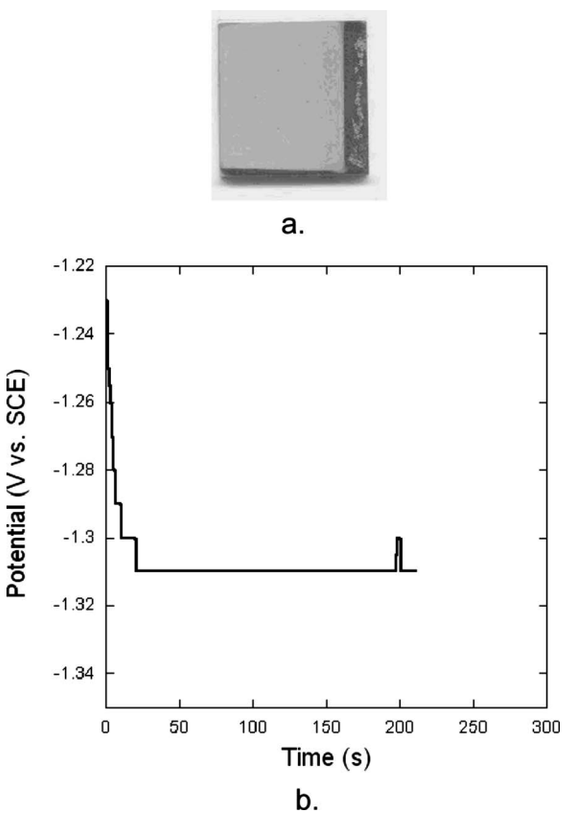

Figure 6. Ag sample deposited with 8 μg/cm^2 NaCl particles after exposure for 22 h to 90% RH with UV radiation but no ozone. (a) Image of exposed sample and (b) galvanostatic reduction curve for exposed sample.

Table II. EDS analysis of corrosion product in atom %. Samples had about 4–6 μg/cm^2 NaCl particles and were exposed for 22 h at 90% RH with UV illumination and two different ozone concentrations.

Element	37 ppm ozone	0.63 ppm ozone
Ag	54.3	71.1
Cl	1.36	1.4
O	28.3	7.9
C	16.1	19.6

Corrosion product analysis.— Ag samples exposed to UV and ozone under wet or dry conditions but with no chloride particles exhibited a corrosion product containing only oxygen and silver as expected.[10] In chloride-deposited samples, the EDS analysis depended on the ozone concentration (Table II). At a very high ozone concentration of 37 ppm, the product was largely oxide with only a small amount of Cl detected. However, at a lower ozone concentration of 0.63 ppm, the corrosion product contained significantly less oxygen.

Effect of exposure time.— An incubation time was found for the corrosion of bare silver in an environment of O_3, RH, and UV, and it was suggested that this process is the result of the chemisorption of OH radical on the bare silver surface.[10] It is of interest to know how the presence of NaCl particles affect the incubation time.

In this set of experiments, Ag samples with about 8 μg/cm^2 NaCl particles were exposed to an environment with UV radiation, 0.633 ppm O_3, and around 90% RH for 0.33, 1, 5, 10, or 22 h. The galvanostatic reduction curves in Fig. 7 show that an incubation time is still required for the corrosion of silver in the presence of NaCl particles as no reduction charge was found after an exposure time of 0.33 h. After 1 h of exposure, the reduction time was about 9 s, and the reduction potential was only about −290 mV_{MSE}. This potential is lower than the normal reduction potential of AgCl, which is from −230 to −260 mV_{MSE}. Furthermore, a level plateau was not observed; the potential decreased with time. A reduction time of about 4.5 s is needed for a reduction of monolayer at 0.1 mA/cm^2, assuming a close-packed Ag plane. Samples exposed for 5, 10, and 22 h exhibited a reduction potential of about −230 mV_{MSE}. The reduction charges for these samples are shown in Fig. 8 along with the data for bare Ag.[10] The corrosion rate, given by the slope of the curve, increased dramatically after the incubation

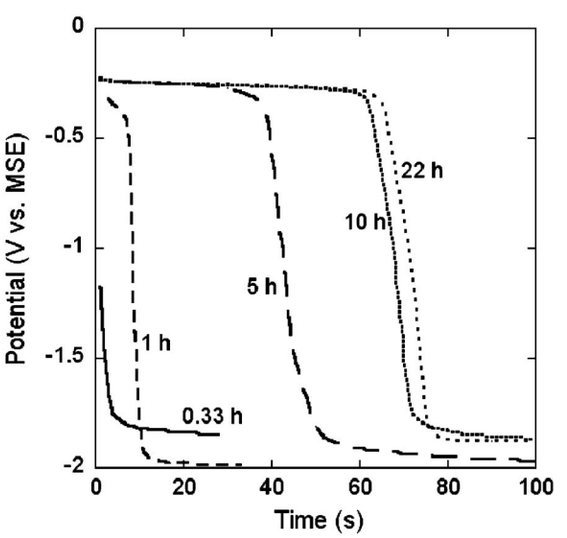

Figure 7. Galvanostatic reduction curves for Ag with 8 μg/cm^2 NaCl exposed to UV, 0.633 ppm O_3, and 90% RH for 0.33, 1, 5, 10, and 22 h.

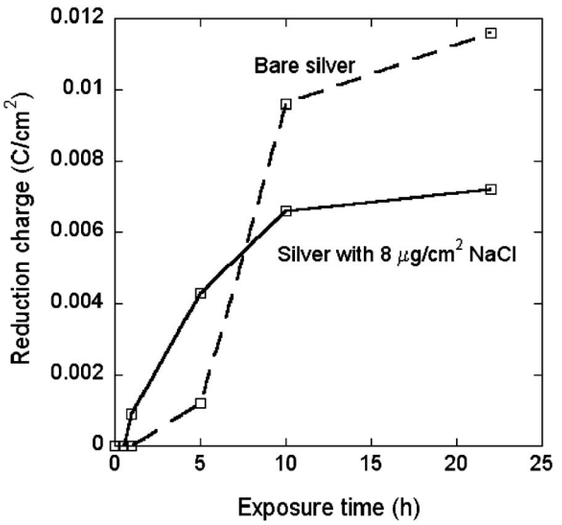

Figure 8. Reduction charge for Ag with 8 $\mu g/cm^2$ NaCl exposed to UV, 0.633 ppm O_3, and 90% RH for 1/3, 1, 5, 10, and 22 h. Data for bare silver shown for comparison.

time and eventually slowed down. This is similar to the reaction for bare silver and is due to the formation of the corrosion product layer, which slows the transport of reactive species. One interesting finding about these experiments is that the incubation time for silver with NaCl particles is shorter than that for bare silver (1 h vs more than 5 h), while the reduction charge for silver with NaCl after 22 h is less than that of bare silver (0.0072 C/cm^2 vs more than 0.01 C/cm^2).

Field-exposed silver samples.— As described in the Experimental section, field-exposed Ag samples were received from various locations across the U.S. Figure 9 shows the SEM images of these samples. All samples exhibited substantial amounts of corrosion product, but the degree of corrosion was not uniform across the surface. The corrosion product morphology depended on the exposure location; some crystalline particles can be observed. Table III provides the elements detected by EDS from these exposure samples. These elements correspond to the usual corrosion products such as AgCl and Ag_2S observed in field exposure tests of silver.[7,32] As was found for the laboratory-exposed samples, a relatively large amount of oxygen is also observed.

The potential transients in Fig. 10a were measured with a saturated calomel electrode (SCE), and those in Fig. 10b were measured with a mercury/mercurous sulfate electrode (MSE). The measured potential difference of MSE relative to SCE was about +381 mV. The average total reduction charges for the various locations are given in Table IV, broken out by the amount associated with each potential plateau or reduction product. The order of increasing amount of corrosion product is 3 months at Maine, 1 month at Lyon Arboretum, HI, 3 months at Point Judith, RI, 1 month at Coconut Island, HI, 3 months at West Jefferson, OH, and 3 months at Daytona Beach, FL. With the exception of the West Jefferson site, the most severe environments were close to the sea, which is reasonable owing to the relatively high RH and salt deposition.

The reduction charge was not reproducible at different spots on the same sample, which is an indication of the complexity of atmospheric corrosion. Two potential plateaus were observed for inland Maine and Point Judith samples: The first plateau at around −250 mV_{MSE} (107 mV_{SCE}) for the Point Judith sample could be due to the presence of AgCl, and the second plateau at around −1122 mV_{MSE} (−700 mV_{SCE}) is the characteristic reduction potential for silver sulfide (Ag_2S). The reduction curve for the West Jefferson, OH sample, which had a large reduction charge, exhibited a plateau at a higher potential, about 250 mV_{SCE}, which is a sign that Ag_2O was present in the corrosion products. A second potential plateau around 107 mV_{SCE} was similar to the reduction potential of AgCl on the Point Judith sample. However, there was no obvious reduction plateau for Ag_2S as observed for the Point Judith or Maine samples. West Jefferson is a semirural suburb of Columbus but might be expected to be exposed to S-polluted air from coal burning power plants in the Midwest. Though silver is extremely susceptible to sulfidation,[3,7] Ag_2S was only observed on Point Judith and Maine samples, suggesting that these two sites have more H_2S and SO_2 contamination. In contrast, AgCl was observed on every sample, and the amount of AgCl was more than Ag_2S. This result could be due to the dominance of salt contamination, especially those close to the sea. It is interesting that the reduction charge at Lyon Arboretum, HI is much less than that at Coconut Island, HI even though these two locations are only separated by 28 km. Lyon Arboretum is in the mountainous rain forest of Oahu. The rain rinses the sample surface of deposited salt species. Field and laboratory studies have indicated that zinc and other surfaces are cleaned of deposited contamination by rain if the amount of rain exceeds about 3 mm.[33,34] Moreover, trees in the mountains can adsorb air pollutants, which may further reduce the amount of reactive species such as O_3 and SO_2.[35]

Salt spray tests on bare silver.— Bare Ag samples (only polished and not deposited with NaCl) were exposed in a salt spray chamber operated according to ASTM B117 for periods ranging from 1 week to 4 months. Figure 11a is a picture of the surface of a freshly polished sample, which was very shiny. The surface of the sample after 1 week in the salt spray chamber still exhibited a shiny surface (Fig. 11b). The sample turned slightly brown after 1 month (Fig. 11c), and a clear brownish film was evident after 4 months of exposure (Fig. 11d). However, the film appeared to be quite thin relative to those formed in the ozone–UV atmosphere after only 22 h, as the polishing marks were still evident on the surface. The galvanostatic reduction curves in Fig. 12 indicated a reduction charge close to zero for all samples, though the curve for the 4 month sample had a reduction time of a few seconds. The low reduction potential for that sample suggests that the product might have been Ag_2S, possibly associated with contamination of the chamber input air.

Discussion

Several interesting observations regarding the effects of UV, RH, and chloride on the corrosion of Ag, as summarized in Fig. 5, are addressed in the following discussion: (*i*) The charge for NaCl-deposited samples at 90% RH with UV was less than that of bare silver at the same condition; (*ii*) the charge at 90% RH with NaCl and UV was similar to that in the dark; (*iii*) the charge at 60% RH with UV and NaCl was lower than that at 90% RH; (*iv*) the charge at 60% RH with NaCl and UV was slightly larger than that in the dark; (*v*) the charge at 60% RH with UV and NaCl was less than that of bare silver at the same condition; (*vi*) the charge at 0% RH in the dark was essentially zero; (*vii*) the charge at 0% RH in UV with NaCl was much more than at 60% RH; and (*viii*) the charge at 0% RH with UV and NaCl was similar to that of bare silver at the same condition.

It is possible to develop a comprehensive mechanistic explanation for the observations by considering the different reactions expected during the laboratory exposure, which can lead to different pathways for the corrosion of silver. A summary of these reactions and the corrosion pathways is given in Fig. 13. First, O_3 can react with chloride in the solution, both in the dark and with UV. Although literature about the reaction between O_3, NaCl, and silver is not available, it is known that O_3 can react with chloride ions in an aqueous solution to form Cl_2, according to Reaction 1.[16] It is likely that the alkaline form of this reaction occurs in the humid environment where the concentration of H^+ is limited

$$H_2O + O_3 + 2Cl^- \rightarrow Cl_2 + 2OH^- + O_2 \quad [5]$$

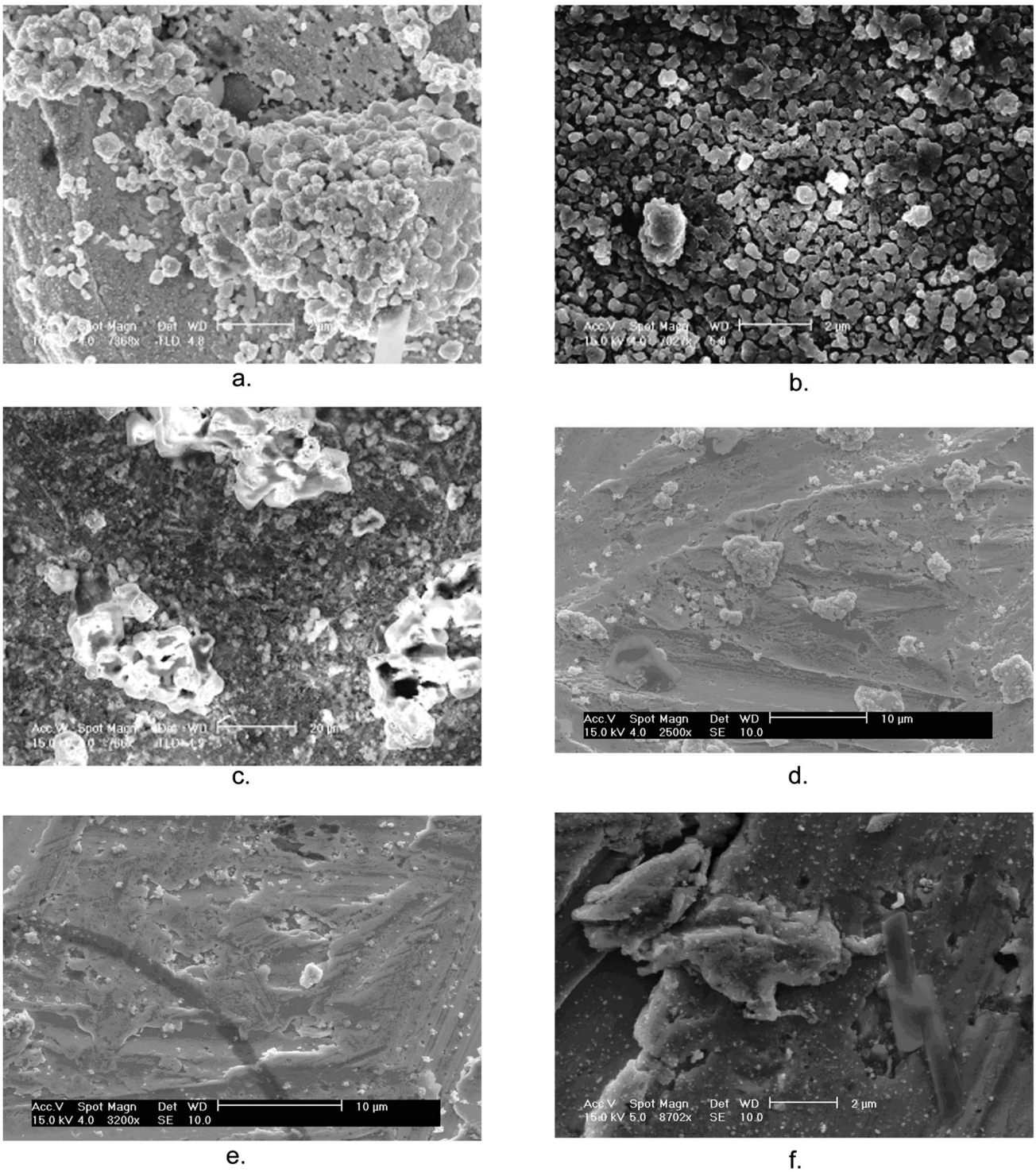

Figure 9. SEM images of sample surfaces after field exposure at various places across the U.S. (a) 3 months exposure at Point Judith, RI. Micrometer marker = 2 μm; (b) 3 months exposure at West Jefferson, OH. Micrometer marker = 2 μm; (c) 3 months exposure at Daytona Beach, FL. Micrometer marker = 20 μm; (d) 1 month exposure at Coconut Island, HI. Micrometer marker = 10 μm; (e) 1 month exposure at Lyon Arboretum, HI. Micrometer marker = 10 μm; (f) 3 months exposure at 3000 ft in inland Maine. Micrometer marker = 2 μm.

The formation of other more oxidized forms of chlorine such as ClO^-, HO_3Cl, and $HOCl^-$ (or $OHCl^-$)[17,18,36] is also possible. For instance, hypochlorite ions can form according to[16]

$$O_3 + Cl^- \rightarrow ClO^- + O_2 \quad [6]$$

The rate of the reaction forming Cl_2, Reaction 1 or 5, is dependent on the pH of the solution, the concentration of catalytic ions,[18] the temperature,[19] and the concentration of dissolved ozone.[20] The decomposition of aqueous ozone can generate some OH radicals, but they are not able to oxidize chloride ions unless the pH is very acidic.[37] Atomic oxygen appears not to be necessary for the fast corrosion of NaCl-contaminated samples in a humid environment. It can be concluded that there is a possible pathway for the corrosion

Table III. Composition from EDS for samples exposed at various sites across the U.S. in wt %.

Element	Point Judith	Central Ohio	Daytona Beach	Coconut Island	Lyon Arboretum	Inland Maine
Ag	89	89	83	89.49	90.96	97.49
C	2.7	2.5	2.3	4.4	4.63	—
O	1.7	5.5	7.8	2.4	2.16	1.13
Cl	5.0	0.39	1.9	1.44	—	0.23
S	1.1	1.3	1.2	0.24	0.22	0.23
Mg	0.46	0.75	2.8	0.79	0.8	0.64
Na	—	—	0.81	1.24	0.4	0.28
Al	—	—	—	—	0.84	—

of silver in an environment containing NaCl, humidity, and ozone, even in the dark, shown as pathway 1 in Fig. 13. Reactive chlorine-containing species, such as Cl_2 or oxyanions such as hypochlorite, generated from the reactions between NaCl, H_2O, and O_3 lead to the generation of the AgCl corrosion product even in the dark

$$Cl_2 + 2Ag \rightarrow 2AgCl \quad [7]$$

The other pathways involve atomic oxygen, which is generated from the photodegradation of ozone by UV of sufficiently low wavelength, according to Reaction 4.

In dry conditions, this atomic oxygen can directly react with silver to form Ag_2O, pathway 2 in Fig. 13

$$O + 2Ag \rightarrow Ag_2O \quad [8]$$

In environments with humidity, the atomic oxygen can react with water to form a hydroxyl radical or peroxide

$$O + H_2O \rightarrow 2\ OH \quad [9]$$

$$O + H_2O \rightarrow H_2O_2 \quad [10]$$

These intermediate products, when present on the Ag surface, react with silver to form Ag_2O, pathway 3 in Fig. 13

$$2\ OH + 2Ag \rightarrow Ag_2O + H_2O \quad [11]$$

A final reaction pathway involves atomic oxygen or hydroxyl radical when present in a sufficiently high concentration, reacting with a chloride solution to form Cl_2 and other chlorine-containing oxyanions, even hypochlorite, for example

$$OH + 2Cl^- \rightarrow Cl_2 + 2\ OH^- \quad [12]$$

Cl_2 results in the formation of AgCl when in contact with Ag, as shown above in Reaction 7. This is reaction pathway 4 in Fig. 13.

Under dry conditions, pathway 2, involving the direct reaction of atomic oxygen and Ag, is the only possibility. However, both O_3 and UV are required for the reaction to occur. Under humid conditions, the other three pathways are possible and are competitive processes. Which of the three pathways dominates and which products form depend on the availability and concentration of the reactive species. Unlike other pathways, pathway 1 does not need UV radiation. With this understanding of the reactions and corrosion pathways, the results presented above can now be addressed.

At 90% RH, which is well above the critical humidity for NaCl deliquescence, a thin layer or microdrops of electrolyte forms in the presence of NaCl. This layer, which is much thicker than that formed on bare Ag at the same RH, slows the reaction by blocking the access of atomic oxygen to the Ag surface. Figure 5 shows that at 90% RH, the reduction charge after 22 h is less with NaCl than for bare Ag. However, as shown in Fig. 8, at 90% RH, the incubation time for the samples with NaCl is shorter, and the initial rate of corrosion is higher than that for the bare samples. For the samples with NaCl, reaction pathways 1, 3, and 4 are possible, and the shorter incubation time is closely related to the thermodynamic stability of AgCl over Ag_2O, which is also supported by the lower reduction potential of AgCl than that of Ag_2O (about -250 mV_{MSE} for AgCl and -130 mV_{MSE} for Ag_2O). As a result, the formation of AgCl is favored over the formation of Ag_2O when both reactive Cl_2 and atomic oxygen are available to the silver surface. For the bare silver with UV, only pathway 3 is available. As a result, the OH radical is able to react with bare silver quickly in the absence of a

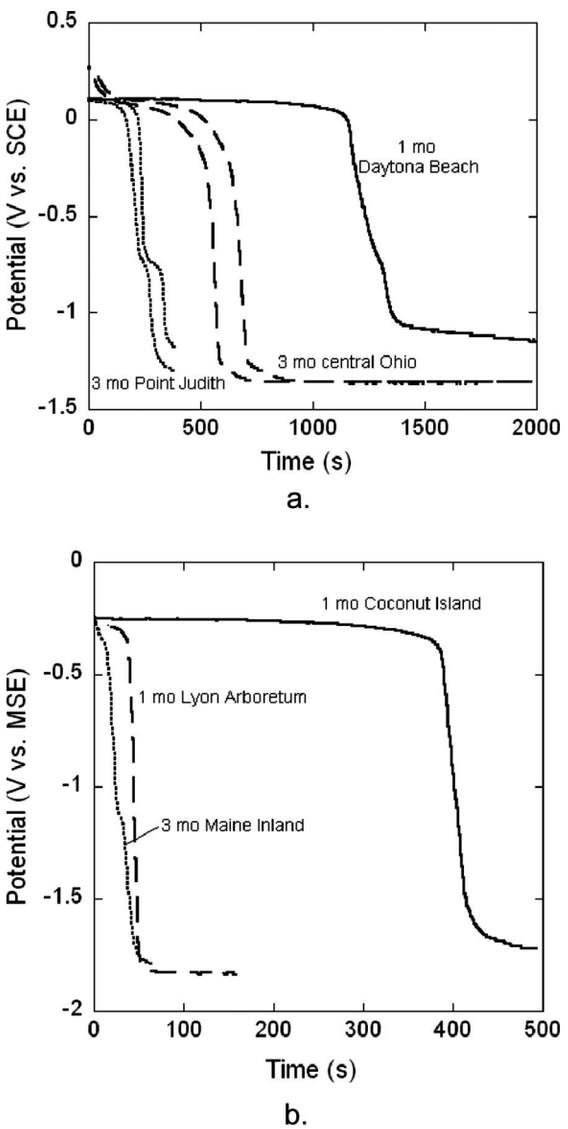

Figure 10. Galvanostatic reduction curves of field-exposure samples at various places. (a) 3 months exposure at Point Judith, RI, 3 months exposure at West Jefferson, OH, and 3 months exposure at Daytona Beach, FL; (b) 1 month exposure at Coconut Island, HI and Lyon Arboretum, HI and 3 months exposure at 3000 ft in inland Maine.

Table IV. Average reduction charges for samples exposed at various sites across the U.S. in C/cm^2.

	Point Judith	Central Ohio	Daytona Beach	Coconut Island	Lyon Arboretum	Inland Maine
	3 months	3 months	3 months	1 month	1 month	3 months
Ag_2O	—	0.005	—	—	—	—
AgCl	0.0216	0.0567	0.1217	0.0401	0.0048	0.0021
Ag_2S	0.009	—	0.011	—	—	0.0022
Total	0.0306	0.0617	0.1327	0.0401	0.0048	0.0043
Extrapolated annual	0.1224	0.2468	0.5308	0.4812	0.0576	0.0172

thick electrolyte layer and competition from Cl_2, which results in more corrosion products even though the incubation time is longer than that for silver with NaCl particles.

The primary reaction mechanism in the presence of NaCl and 90% RH seems to be pathway 1 where ozone is solvated directly into the thick chloride layer by water molecules, oxidizing the chloride and resulting in AgCl formation. This assertion is supported by the observation that the reduction charge was essentially the same with and without UV in this case. At higher O_3 concentrations, UV radiation possibly has a larger effect by generating more atomic oxygen so that pathway 4 would be more prominent. Furthermore, as the amount of NaCl on the surface decreases or as the amount of ozone increases, the amount of generated Cl_2 lessens and pathway 3 is favored over 1 and 4.

The EDS analysis of exposed samples in Table II generally supports the described reaction pathways. The corrosion product for samples exposed to high ozone concentrations exhibited high oxygen content, and the amount of oxygen decreased as the ozone concentration decreased. The reduction potential also depended on the ozone concentration. For exposure in 37 ppm ozone, the reduction potential in deaerated pH 10 0.1 M Na_2SO_4 solution was about 250 mV SCE or about −130 mV MSE. In contrast, the corrosion product formed in 0.63 ppm ozone reduced at about −250 mV MSE, which is characteristic of the potential for AgCl reduction.[10] The reduction potential reflects the presence of AgCl for the 0.63 ppm ozone although the chlorine concentration determined by EDS is much lower

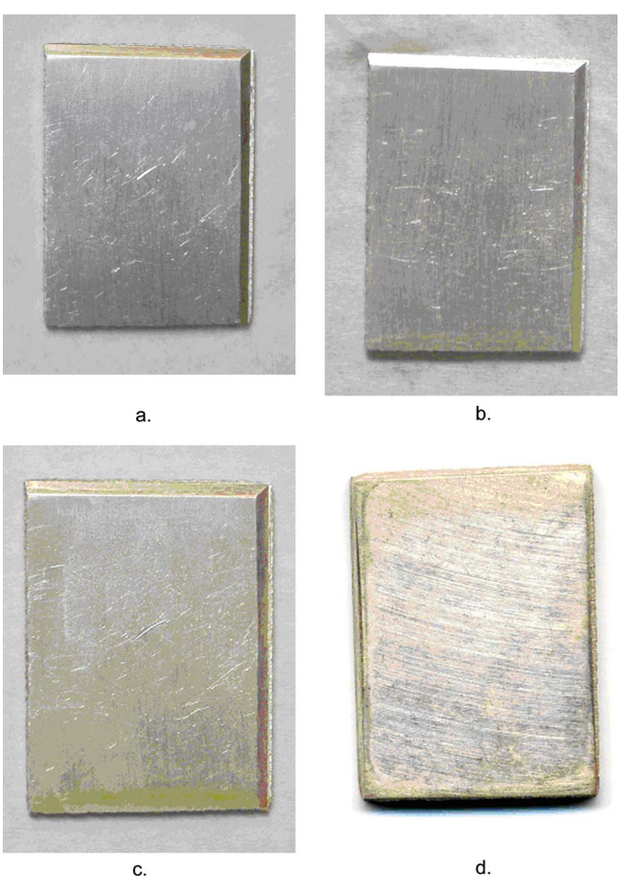

Figure 11. (Color online) Pictures of sample surface after salt spray tests. (a) Freshly polished, (b) after 1 week of exposure, (c) after 1 month of exposure, and (d) after 4 months of exposure.

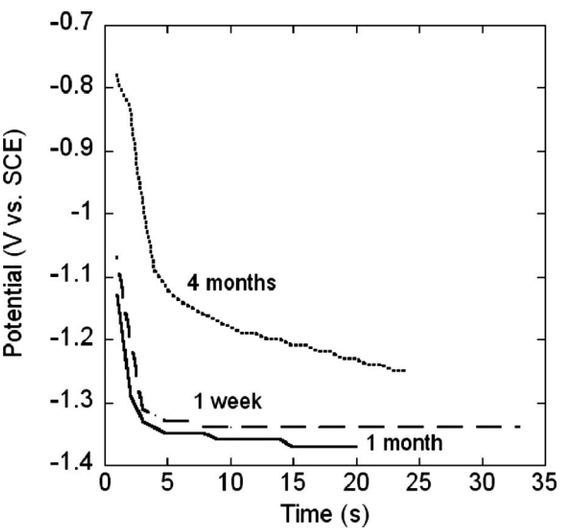

Figure 12. Galvanostatic reduction curve for silver samples exposed in salt spray environment from 1 week to 4 months.

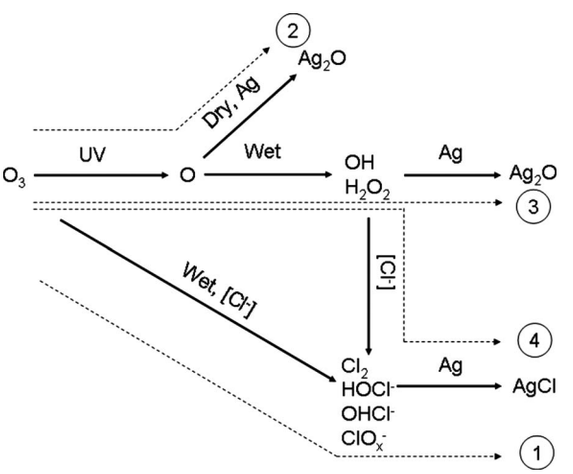

Figure 13. Possible reactions with O_3 and reaction pathways of Ag corrosion given as dashed lines.

than that of oxygen. The reduction potential and composition, other than S, are similar for the laboratory- and field-exposed samples. This indicates that the corrosion product is similar so that the laboratory tests are relevant accelerations of the field, which are discussed further below.

At 60% RH, which is below the NaCl deliquescence RH, only a thin adsorbed water layer is present on the surface. However, the reduction charge in the presence of NaCl is less than that for bare Ag. Furthermore, the charge with UV is only slightly higher than that in the dark for samples with NaCl particles. One other important factor is the reduction potential, which indicates that the corrosion product layer is AgCl, not Ag_2O. These observations indicate that even though the NaCl particles do not deliquesce, there is an interaction with the humid environment to create reactive chlorine-containing species, such as Cl_2 and oxyanions such as hypochlorite. In fact, corrosion of copper has been observed at 55% RH in the presence of NaCl particles.[38] The important reaction pathways seem to be 1 and 4, as was the case for the deliquesced surface at 90% RH. However, at 60% RH, the reduction charge is slightly higher with UV, indicating a stronger contribution of pathway 4 than at 90% RH. The reduction charges at 60% RH are less than that at 90% RH both in the dark and with UV. This result is expected because the reaction rate of pathway 1 decreases as water becomes less available when the RH drops. Less corrosion product was also observed compared to bare silver with UV at 60% RH. RH has little effect on the reduction charge of bare silver because the chemisorption process of the OH radical in pathway 3 is barely influenced by the presence of a thin layer of adsorbed water.[10] However, in the presence of NaCl, AgCl forms faster and blocks the reaction to oxide, as shown in Fig. 8. Similar to the expectation at 90% RH, the effect of UV becomes more obvious at a higher ozone concentration and a lower amount of NaCl.

At 0% RH in dark conditions, the absence of water on the sample surface prevents the reactions between the ozone and chloride described above, so there is no corrosion product. However, when UV radiation and ozone are both present, atomic oxygen is generated and reacts strongly with silver even at 0% RH, as shown in pathway 2. This reaction is extremely rapid under dry conditions where atomic oxygen has unhindered access to the sample surface similar to pathway 3. The charge for NaCl-deposited Ag is about the same as for the bare Ag sample because the chloride particles are essentially inert due to the absence of water at dry conditions. This charge is larger than that at 60 and 90%, which is due to the lack of competition from Cl_2 and the formation of AgCl at dry conditions.

The reduction potential of samples with NaCl at different RH values in the dark and with UV radiation (except 0% RH in dark where there is no corrosion product) is around -250 mV_{MSE}, which is a characteristic potential for AgCl. It is expected that the corrosion product in 0% RH with UV would not contain AgCl, so it is surprising that the potential of AgCl is observed. However, it is possible that dissolution into the solution of the unreacted NaCl particles on the Ag surface when the sample is immersed in the reduction solution results in an environment that converts Ag_2O to AgCl on the surface. Such reaction has been previously observed.[10] Once the product is converted to chloride, the reduction potential of NaCl is observed.

The laboratory exposure results show that the combination of UV radiation, ozone, humidity, and chloride can result in rapid Ag corrosion. The role of ozone is dominant as the phenomenon is not observed in the absence of ozone. UV can have an effect if the ozone concentration is relatively high when the amount of NaCl is limited, and the RH is below the deliquescence RH. However, if the ozone concentration is relatively low, the amount of NaCl is relatively high, and the RH is relatively high, the effect of UV is not obvious as pathway 1 becomes dominant. In the field exposure, where ozone concentrations are even lower than our laboratory condition (20–80 ppb in the field compared to 630 ppb in the laboratory) and RH is constantly present, it can be expected that UV radiation would not have a large effect. Because a salt spray chamber is in the dark, pathway 1 is the only one of the four available. Furthermore, in standard salt spray cabinets, the air is filtered to remove particles above 5 μm and is passed through water and then the 0.5 M NaCl solution. These steps probably remove gaseous accelerating agents such as O_3, H_2S, and SO_2. As a result of this and the darkness, the extent of reaction on the silver surface is extremely low in the salt spray chamber.

It is generally accepted that the corrosion rate of field-exposure samples decreases with decreasing RH.[2-4] Although the laboratory exposure of bare silver did not exhibit RH dependence in the presence of UV, which is due to the independence of the initial chemisorption process and direct oxidation by atomic oxygen or OH radical at dry or wet condition, the laboratory exposure of silver with chloride at wet conditions clearly showed a strong RH dependence both in the dark and with UV. This is an indication of a good correlation between field and laboratory exposures. However, as indicated in the laboratory exposure of silver with chloride at dry conditions with UV, independence of RH can be expected as pathway 2 (formation of atomic oxygen, which reacts with silver directly to generate Ag_2O) dominates.

An estimation of the acceleration factor in the laboratory exposure can be made by linear extrapolation of the results to longer times even though Fig. 8 shows that the reaction is not exactly linear with time. Table IV shows extrapolated annual reduction charges for the field samples exposed at the various locations. The most severe sites (as evidenced by the largest reduction charges) are Daytona Beach and Coconut Island, which are expected because they are beach sites. The standard laboratory exposure, with about 8 $\mu g/cm^2$ NaCl particles, UV irradiation, 0.633 ppm O_3, and 90% RH, resulted in about 0.006 C/cm^2 after 22 h, which extrapolates to about 2.4 C/cm^2 after 1 year. The acceleration factor is therefore about 5 relative to the beach sites and larger for the inland sites.

Although the O_3 concentration of 0.63 ppm is very low compared to other previous laboratory exposures, it is still higher than the O_3 concentration in the field, which is usually from 0.02 to 0.08 ppm.[39] Additionally, the UV intensity from sunlight at sea level, less than 1 mW/cm^2,[40] is less than the UV intensity in the laboratory exposure, 4 mW/cm^2. Certainly, the intensity of 254 nm radiation in the laboratory was much greater than that in the field because light of wavelength less than 290 nm typically does not reach the earth's surface. Based on our laboratory exposure results, pathway 3 (UV breaks O_3 bond to form atomic oxygen, which reacts with bare Ag to form Ag_2O) becomes dominant in places with little deposition of sea-salt particles (i.e., places far away from the sea). Pathways 1 and 4 become more dominant in places where sea-salt particles are more abundant (i.e., places close to the sea). The effectiveness of pathway 4 depends on the O_3 concentration, the RH, and the UV intensity. Pathway 4 increases the corrosion rate if it is present.

Part of the problem of accelerating the field-exposure condition is knowing the corrosion products that form in the field and the controlling factors for the formation of those products so that they can be replicated. Tables III and IV provide two different descriptions of the nature of the corrosion product formed on Ag at a variety of outdoor locations. The EDS data are determinative, showing exactly what was on the sample surfaces. However, the depth of the excitation volume makes the EDS data from surface films qualitative rather than quantitative. The reduction charges are quantitative, but the plateaus relate broadly to the nature of the product layer. The samples exposed near the ocean all exhibited reduction plateaus for AgCl rather than Ag_2O, but the EDS data showed considerable amounts of O and sometimes more O than Cl. The results of the laboratory testing would have predicted that the corrosion product for the likely conditions in central Ohio (low chloride relative to the beach exposures) would result in the formation of Ag_2O via pathway 3. The reduction curves for central Ohio exhibited Ag_2O, but much more AgCl, and in fact, the charge associated with AgCl was larger than for some of the samples exposed near the ocean. The stability of Ag oxides, of course, depends on the surface pH as they become soluble at low pH values.[41] However, the

amount of Cl from EDS was quite low, and the amount of O was high on that sample. Similarly, the presence of S in the EDS data did not correlate well with the presence of a plateau for Ag_2S. Clearly, these data and the images of the corrosion product indicate that the corrosion products formed in the atmosphere are quite complicated. There is a need to characterize those products more fully in terms of structure and composition and to know how to replicate them in the laboratory.

Conclusions

The reaction of Ag in environments containing ozone, humidity, NaCl particles, and UV light was studied. The following was found:

1. Nanometer-sized NaCl particles were successfully deposited on a silver surface using a thermophoretic deposition instrument.
2. Experiments in an ESEM revealed that nanometer-sized NaCl particles started to deliquesce at 80% RH. At high RH, a layer of electrolyte was observed but was not uniform across the surface. Larger NaCl crystals formed when the RH was decreased below 75% RH.
3. Ag deposited with NaCl particles corrodes rapidly in an environment with ozone, RH, and UV light. Corrosion also occurs in the dark, except under dry conditions. In the presence of humidity, the rate of corrosion is not strongly influenced by UV light but does depend on the RH.
4. An incubation time is needed for the initiation of Ag corrosion with NaCl particles. However, the incubation time is shorter than that of bare silver because the formation of AgCl is favored over the formation of Ag_2O when both reactive Cl_2 and OH radical are available to the silver surface.
5. The amount of corrosion products on silver with NaCl particles after 22 h in an environment with ozone, RH, and UV is less than that of bare silver because of the presence of a thick electrolyte layer and competition from Cl_2.
6. Four different reaction pathways for Ag in environments containing varying ozone, UV light, humidity, and NaCl particles were proposed. The amount of corrosion product observed after 22 h depends on the competition between these pathways.
7. In the presence of NaCl particles and humidity, fast corrosion can occur without UV light because of the formation of Cl_2 and other oxidized Cl species from the reaction between O_3 and chloride ion. This results in the formation of AgCl. The reduction charge decreases with decreasing RH because this pathway depends on the availability of water.
8. In the presence of NaCl particles and RH less than the critical RH, the reduction charge is higher with UV than in the dark because of the additional pathway involving the generation of Cl_2 and other oxidized Cl species from the reaction of OH and chloride ion.
9. In the presence of NaCl particles and humidity, the reduction charge is less than that for bare Ag because the Cl_2 and other oxidized Cl species result in the formation of AgCl and block OH from the surface.
10. Ag samples exposed at different outdoor locations across the U.S. corroded to varying extents. Three months of exposure at Daytona Beach, FL exhibited the most severe atmospheric attack, while the sample exposed for 3 months at an inland Maine site showed the least corrosion attack.
11. Little corrosion product formed on Ag in a salt spray chamber even after 4 months of exposure in contrast to what is observed in the field-exposure tests. The chamber is dark and the input air contains no reactive species such as ozone, so corrosion is slow.

Acknowledgments

This work was supported by contracts from D. Dunmire at the U.S. Office of the Secretary of Defense through Mandaree Enterprise Corp. The guidance and input of W. Abbott and R. Kinzie are greatly appreciated. Furthermore, Dr. Abbott graciously provided samples that had been exposed at various outdoor locations.

Ohio State University assisted in meeting the publication costs of this article.

References

1. F. Deflorian, S. Rossi, L. Fedrizzi, and C. Zanella, *Prog. Org. Coat.*, **59**, 244 (2007).
2. H. Bennett, R. Peck, D. Burge, and J. Bennett, *J. Appl. Phys.*, **40**, 3351 (1969).
3. H. Kim, *Mater. Corros.*, **54**, 243 (2003).
4. M. Forslund, J. Majoros, and C. Leygraf, *J. Electrochem. Soc.*, **144**, 2637 (1997).
5. L. Volpe and P. Peterson, *Corros. Sci.*, **29**, 1179 (1989).
6. L. Volpe and P. Peterson, in *First International Symposium on Corrosion of Electronic Materials and Devices*, J. D. Sinclair, R. P. Frankenthal, R. L. Opila, and J. H. Payer, Editors, PV 91-2, p. 22, The Electrochemical Society Proceedings Series, Pennington, NJ (1991).
7. D. Rice, P. Peterson, E. Rigby, P. Phipps, R. Cappell, and R. Tremoureux, *J. Electrochem. Soc.*, **128**, 275 (1981).
8. T. Graedel, *J. Electrochem. Soc.*, **139**, 1963 (1992).
9. Y. Fukuda, T. Fukushima, A. Sulaiman, I. Musalam, L. Yap, L. Chotimongkol, S. Judabong, A. Potjanart, O. Keowkangwal, K. Yoshihara, et al., *J. Electrochem. Soc.*, **138**, 1238 (1991).
10. Z. Chen, D. Liang, G. Ma, G. S. Frankel, H. C. Allen, and R. G. Kelly, *Corros. Eng., Sci. Tech.*, Accepted for publication.
11. T. Shinohara, S. Motoda, and W. Oshikawa, in *Pricm 5: The Fifth Pacific Rim International Conference on Advanced Materials and Processing, Pts 1-5*, Z. Y. Zhong, H. Saka, T. H. Kim, E. A. Holm, Y. F. Han, and X. S. Xie, Editors, Trans Tech, Uetikon-Zurich, Switzerland, p. 61 (2005).
12. I. S. Cole, N. S. Azmat, A. Kanta, and M. Venkatraman, *Int. Mater. Rev.*, **54**, 117 (2009).
13. R. Irshad, R. Grainger, D. Peters, R. McPheat, K. Smith, and G. Thomas, *Atmos. Chem. Phys.*, **9**, 221 (2009).
14. W. C. Keene, R. Sander, A. A. P. Pszenny, R. Vogt, P. Crutzen, and J. Galloway, *J. Aerosol Sci.*, **29**, 339 (1998).
15. U. von Gunten, *Water Res.*, **37**, 1469 (2003).
16. L. Yeatts and H. Taube, *J. Am. Chem. Soc.*, **71**, 4100 (1949).
17. R. D'Auria, W. Kuo, and D. J. Tobias, *J. Phys. Chem. A*, **112**, 4644 (2008).
18. A. Levanov, I. Kuskov, K. Koiaidarova, A. Zosimov, E. Antipenko, and V. Lunin, *Kinetics and Catalysis*, **46**, 138 (2005).
19. A. Levanov, I. Kuskov, A. Zosimov, E. Antipenko, and V. Lunin, *Kinet. Catal.*, **44**, 740 (2003).
20. A. Levanov, I. Kuskov, E. Antipenko, and V. Lunin, *Russ. J. Phys. Chem.*, **82**, 2045 (2008).
21. M. E. Lovato, C. A. Martin, and A. E. Cassano, *Chem. Eng. J. (Lausanne)*, **146**, 486 (2009).
22. H. Lu and D. Duquette, *Corrosion (Houston)*, **46**, 843 (1990).
23. M. Gurol and A. Akata, *AIChE J.*, **42**, 3283 (1996).
24. G. Peyton and W. Glaze, *Environ. Sci. Technol.*, **22**, 761 (1988).
25. H. Taube, *Z. Rheumaforsch*, **53**, 209 (1957).
26. I. Wagner, J. Karthaeuser, and H. Strehlow, *Ber. Bunsenges. Phys. Chem.*, **90**, 861 (1986).
27. E. Knipping, M. Lakin, K. Foster, P. Jungwirth, D. Tobias, R. Gerber, D. Dabdub, and B. Finlayson-Pitts, *Science*, **288**, 301 (2000).
28. K. Oum, M. Lakin, D. DeHaan, T. Brauers, and B. Finlayson-Pitts, *Science*, **279**, 74 (1998).
29. B. Finlayson-Pitts and J. Pitts, *Chemistry of the Upper and Lower Atmosphere*, Academic, San Diego (2000).
30. G. Nishio, S. Kitani, and K. Takahashi, *Ind. Eng. Chem. Process Des. Dev.*, **13**, 408 (1974).
31. G. Biskos, A. Malinowski, L. M. Russell, P. R. Buseck, and S. T. Martin, *Aerosol Sci. Technol.*, **40**, 97 (2006).
32. M. Watanabe, A. Hokazono, T. Handa, T. Ichino, and N. Kuwaki, *Corros. Sci.*, **48**, 3759 (2006).
33. I. S. Cole, W. D. Ganther, and D. Lau, *Corros. Eng., Sci. Tech.*, **41**, 310 (2006).
34. I. S. Cole, D. Lau, F. Chan, and D. A. Paterson, *Corros. Eng., Sci. Tech.*, **39**, 333 (2004).
35. W. Smith, *Air Pollution and Forests Interactions Between Air Contaminants and Forest Ecosystems*, Springer, New York (1982).
36. E. Knipping and D. Dabdub, *J. Geophys. Res., [Atmos.]*, **107**, 4360 (2002).
37. J. Hoigne, *Sci. Total Environ.*, **47**, 169 (1985).
38. Z. Chen, S. Zakipour, D. Persson, and C. Leygraf, *Corrosion (Houston)*, **60**, 479 (2004).
39. J. Schwab, J. Spicer, and K. Demerjian, *J. Air Waste Manage. Assoc.*, **59**, 293 (2009).
40. *Annual Book of ASTM Standards*, ASTM, Philadelphia, PA (2003).
41. M. Pourbaix, *Atlas of Electrochemical Equilibrium in Aqueous Solutions*, Pergamon, Oxford, NY (1976).